

Mesoscopic fluctuations in the spin-electric susceptibility due to Rashba spin-orbit interaction

Mathias Duckheim and Daniel Loss

Department of Physics University of Basel, CH-4056 Basel, Switzerland

(Dated: November 23, 2018)

We investigate mesoscopic fluctuations in the spin polarization generated by a static electric field and by Rashba spin-orbit interaction in a disordered 2D electron gas. In a diagrammatic approach we find that the out-of-plane polarization – while being zero for self-averaging systems – exhibits large sample-to-sample fluctuations which are shown to be well within experimental reach. We evaluate the disorder-averaged variance of the susceptibility and find its dependence on magnetic field, spin-orbit interaction, dephasing, and chemical potential difference.

PACS numbers: 72.25.Dc, 73.23.-b, 85.75.-d, 75.80.+q

A primary goal in semiconductor spin physics is the control of magnetic moments by electric fields [1, 2]. One way to achieve this is to make use of the magnetoelectric effect (MEE) [3, 4], a spin polarized steady state which emerges from intrinsic ‘magnetic’ fields generated by spin-orbit interactions (SOI) and transport. While this MEE has been observed e.g. in n-InGaAs epilayers [5, 6, 7] and hole gases [8], the resulting net polarization is below percent for electron systems [5, 7], and thus much smaller than what has been achieved by optical pumping [6, 9, 10]. Moreover, in a standard two-dimensional electron gas (2DEG), with typical Rashba SOI [11], the MEE generates only in-plane spin polarization but no out-of-plane components [4]. The latter would be desirable, also since they can be detected more easily e.g. by optical means.

However, these observations apply only to disordered phase-incoherent systems with self-averaging [12]. On the other hand, it is well-known that phase-coherence in mesoscopic systems leads to new quantum effects such as conductance fluctuations or weak antilocalization, especially due to intrinsic SOI [13, 14, 15, 16, 17, 18].

Similarly, mesoscopic spin effects emerge for the MEE when the system becomes phase-coherent. Indeed, focussing on 2DEGs with Rashba SOI, we will show here that the spin-electric susceptibility is subject to strong sample-to-sample fluctuations, and thus individual mesoscopic samples with phase coherence can exhibit a large net spin polarization. Quite remarkably, these strong fluctuations show up not only in the in-plane but also in the out-of-plane spin components. We find that these fluctuations considerably exceed the polarization obtained in self-averaging samples, and since the latter has been successfully measured by optical means [5, 7], the spin fluctuations predicted here should be well within experimental reach. We will see that this strong enhancement is special for Rashba (or Dresselhaus[29]) SOI, and, diagrammatically, it results from a spin vertex renormalization typical for such intrinsic SOI [4, 19, 20].

Related effects studied before are local spin fluctuations in metallic conductors due to the extrinsic spin-

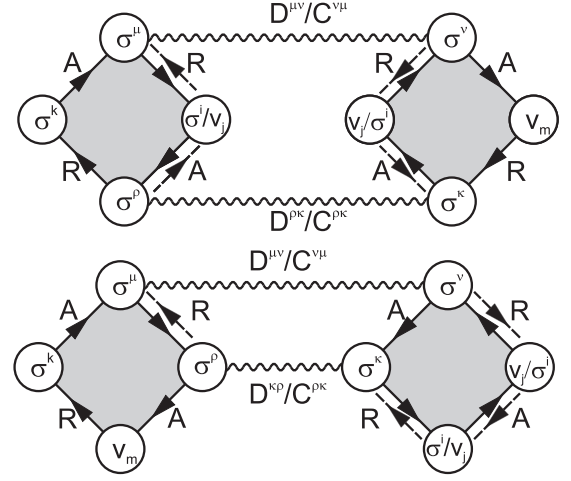


FIG. 1: Dominant diagrams (for $1/pFl \ll 1$) leading to the variance $\overline{\delta\chi^{ij}\delta\chi^{km}}$ given in Eq. (3), see also Fig. 2. The upper diagram contains the Hikami boxes (HB) V_{La}, V_{Ra} (with solid arrows and two Diffusons (D)) and V_{Ld}, V_{Rd} (with dashed arrows and two Cooperons (C)), *resp.* The lower diagram contains the HBs V_{Lb}, V_{Rb} (solid arrows, two Diffusons) and V_{Lc}, V_{Rc} (dashed arrows, two Cooperons).

orbit effect [21] (as opposed to the intrinsic Rashba SOI [22]), density of states fluctuations of quantum corrals [23], and fluctuations of spin currents in general nanostructures [24] and chaotic quantum dots [24, 25]. While thermal spin fluctuations have been observed [26], we are not aware of studies of mesoscopic spin fluctuations due to the MEE as described here.

We consider a disordered mesoscopic square-shaped 2DEG of size L^2 containing non-interacting electrons of mass m and charge e and described by the Hamiltonian

$$H = \frac{\mathbf{p}^2}{2m} + \alpha(p_1\sigma^2 - p_2\sigma^1) + \mathbf{b} \cdot \boldsymbol{\sigma} + V. \quad (1)$$

Here, $\mathbf{p} = (p_1, p_2, 0)$ is the in-plane momentum, α the Rashba SOI constant [11], $2b = g\mu_B B(\cos\varphi_B, \sin\varphi_B, 0)$ an external in-plane magnetic field, and $\boldsymbol{\sigma} = (\sigma^1, \sigma^2, \sigma^3)$ the Pauli matrices (and $\sigma^0 = \mathbb{1}$). The disorder po-

tential V is due to static short-ranged impurities randomly distributed and characterized by the mean free path $l = \tau p_F/m$, where τ is the scattering time and p_F the Fermi momentum.

The spin polarization due the MEE is given in linear response by $\langle \sigma^i \rangle = \chi^{ij} E_j$, $i = 1, 2, 3$, where E_j is a static electric field applied along the j -direction and χ^{ij} the (zero-frequency) spin-electric susceptibility (per unit area). Here, we focus on the mesoscopic fluctuations of χ^{ij} due to disorder, described by the variance $\overline{(\delta\chi^{ij})^2}$, where $\delta\chi^{ij} = \chi^{ij} - \overline{\chi^{ij}}$ and where the overbar denotes disorder averaging. We start from the Kubo formula for χ^{ij} expressed in terms of retarded/advanced Green functions $G_{E_F}^{R/A}$ at the Fermi energy E_F [19]

$$\chi^{ij}(E_F) = \frac{e}{4\pi} \text{Tr} \sigma^i (G_{E_F}^R - G_{E_F}^A) v_j (G_{E_F}^R - G_{E_F}^A), \quad (2)$$

where $\text{Tr} \rightarrow \int d^2p/(2\pi)^2 \text{tr}_S$ denotes momentum integration and spin trace, and $v_j = i[H, x_j]/\hbar$ is the SOI-dependent velocity operator. In Eq. (2) we have used time reversal invariance [30] to make the symmetry $\chi^{ij} = \chi^{ji}$ explicit [31].

The variance $\overline{(\delta\chi^{ij})^2}$ is obtained as the impurity average over the product of two susceptibilities given in Eq. (2). Extending the diagrammatic approach of [4, 12, 14] to include SOI and spin vertices, we obtain the diagrams shown in Fig. 1 which give the dominant contribution to the variance for $1/pFl \ll 1$. Explicitly, we find

$$\begin{aligned} \overline{\delta\chi^{ij}(E_F + \Delta) \delta\chi^{km}(E_F)} &= \left(\frac{e}{2\pi L} \right)^2 \int \frac{d^2q}{(2\pi)^2} \left[\right. \\ &V_{La}^{\mu\rho} V_{Ra}^{\kappa\nu} D_{-q}^{\mu\nu}(\Delta) D_q^{\rho\kappa}(-\Delta) + V_{Lb}^{\mu\rho} V_{Rb}^{\kappa\nu} \{ D_q^{\mu\nu}(\Delta) D_q^{\rho\kappa}(\Delta) \\ &+ D_q^{\mu\nu}(-\Delta) D_q^{\rho\kappa}(-\Delta) \} + V_{Lc}^{\mu\rho} V_{Rc}^{\kappa\nu} \{ C_q^{\nu\mu}(\Delta) C_q^{\rho\kappa}(q, \Delta) \\ &+ C_q^{\nu\mu}(-\Delta) C_q^{\rho\kappa}(-\Delta) \} + V_{Ld}^{\mu\rho} V_{Rd}^{\kappa\nu} C_q^{\mu\nu}(-\Delta) C_q^{\rho\kappa}(\Delta) \left. \right]. \quad (3) \end{aligned}$$

Here, Δ is the difference in chemical potentials or gate voltages of χ^{ij} and χ^{km} , and D_q and C_q are the Diffuson and Cooperon matrices, resp., with 4×4 components $\mu, \nu = 0, 1, 2, 3$ (see below). The V_{La} 's (V_{Ra} 's) are Hikami

boxes (HBs) shown on the left (right) in Fig. 1. Since $\chi^{ij} = \chi^{ji}$ (see Eq. (2)), each product $V_L^{\mu\rho} V_R^{\kappa\nu}$ in Eq. (3) turns into a sum with 4 terms. These terms are obtained by exchanging spin and velocity vertices in the V 's such as e.g. $V_{La}^{\mu\rho} V_{Ra}^{\kappa\nu} \equiv V_{La}^{\mu\rho}[\sigma^i, \sigma^k] V_{Ra}^{\kappa\nu}[v_j, v_m] + (\sigma^k \leftrightarrow v_m) + (\sigma^i \leftrightarrow v_j) + (\sigma^k \leftrightarrow v_m, \sigma^i \leftrightarrow v_j)$. Additionally, the vertices have to be dressed with non-crossing impurity lines ([19, 20]). In contrast to conductance fluctuations [12, 14], such vertex corrections are crucial here as they give the dominant dependence on the SOI (see below).

Let us now evaluate Eq. (3) by calculating first $V_{L/R}$, given in Fig. 1, and then C/D . From now on, we restrict ourselves to the diffusive regime $l/L \ll x = 2\alpha p_F \tau \ll 1$, which allows us to neglect the q -dependence in $V_{L/R}$ and to expand in x . Additionally, we may neglect b and Δ in $V_{L/R}$. Indeed, we first note that $V_{b \neq 0}/V_{b=0} \propto b\tau$ and $V_{\Delta \neq 0}/V_{\Delta=0} \propto \Delta\tau$ for small b and Δ , and second, that the suppression of C/D with increasing b and Δ sets in on a much smaller scale $b\tau \approx \sqrt{\phi x^2}$ and $\Delta\tau \approx \phi$ (dephasing, see below). As a result, we can unify the calculation of

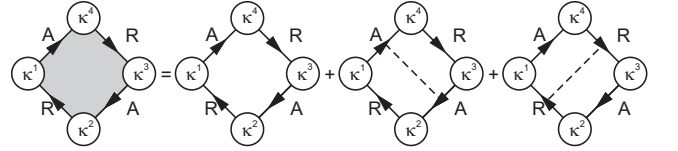


FIG. 2: General Hikami box (HB): shaded area represents the correction to the 'empty' box V_a by V_b, V_c containing a single impurity line (dashed). The vertices are denoted by $\kappa^i \in \{\sigma^\mu, v_1, v_2\}$, and R/A stands for the averaged $G_{E_F, b}^{R/A}$.

the $2 \times 4 \times 4$ HBs in Fig. 1. They can be expressed by a linear relation [32] in terms of the general HB in Fig. 2, defined by the 'empty' box $\text{Tr} \{ G^A \kappa^1 G^R \kappa^2 G^A \kappa^3 G^R \kappa^4 \}$ and the associated HBs with a single impurity line. Here, $\kappa^i \in \{\sigma^\mu, v_1, v_2\}$ denotes vertices in Figs. 1, 2, and in Eq. (3), and $G_{E_F, b}^{R/A}(\mathbf{p})$ is the impurity averaged Green function which depends on B-field and SOI [19].

Next, we evaluate the Diffuson D and Cooperon C in Eq. (3), given by $D_q = (1/2m\tau)(1 - X_+)^{-1}$ and $C_q = (1/2m\tau)k(1 - X_-)^{-1}k$, where $k^{\mu l} = \text{tr}\{\sigma^2 \sigma^\mu \sigma^l\}/2$. Expanding $X_{\pm}^{\mu\nu} = \text{Tr}\{\sigma^\mu G_{E_F, b}^R(\mathbf{p}) \sigma^\nu G_{E_F, \pm b}^A(\mathbf{p} - \mathbf{q})\}/2m\tau$ in $\bar{q} = ql \ll 1$, $\beta = 2b\tau \ll 1$, and x , we find

$$X_\epsilon = \begin{pmatrix} \frac{1}{\lambda} - \frac{\bar{q}^2}{2} - \beta^2 \delta_{\epsilon, -1} & -i\beta \delta_{\epsilon, -1} & 0 & 0 \\ -i\beta \delta_{\epsilon, -1} & \frac{1}{\lambda} - \frac{\bar{q}^2}{2} - \frac{x^2}{2} - \beta^2 \delta_{\epsilon, -1} & 0 & ix\bar{q} \cos \varphi \\ 0 & 0 & \frac{1}{\lambda} - \frac{\bar{q}^2}{2} - \frac{x^2}{2} - \beta^2 \delta_{\epsilon, +1} & -\beta \delta_{\epsilon, +1} + ix\bar{q} \sin \varphi \\ 0 & -ix\bar{q} \cos \varphi & \beta \delta_{\epsilon, +1} - ix\bar{q} \sin \varphi & \frac{1}{\lambda} - \frac{\bar{q}^2}{2} - x^2 - \beta^2 \delta_{\epsilon, +1} \end{pmatrix}, \quad (4)$$

where φ is the polar angle of the momentum $\bar{\mathbf{q}}$ and

$\lambda = 1 - i\Delta\tau$. We will find below that the main contribu-

tion to $\overline{\delta\chi^2}$ comes from the $1/\bar{q}^2$ terms in D^{00} and C^{33} . To account for orbital dephasing we introduce a corresponding dephasing time τ_ϕ in D and C by the standard replacement (see e.g. Eq.(3.15) in [27]) $\Delta \rightarrow \Delta + i/\tau_\phi$.

Although generalized to include spin vertices, the method presented so far involves the calculation of similar diagrams as for the conductance fluctuations [12, 13]. An important difference, however, is the inclusion of the vertex corrections for spin and spin-dependent velocity which we discuss now. The vertex correction is an infinite sum of diagrams which consists of non-crossing impurity lines connecting the retarded and advanced Green functions in either χ^{ij} or χ^{km} , *resp.* For the velocity vertex this leads to $v_j \rightarrow p_j/m$, i.e. the spin part of the velocity is cancelled in the dc limit [20]. For the spin vertex this leads to the replacement $\sigma^i \rightarrow \Sigma^{i\mu}\sigma^\mu$ where Σ is diagonal given by $\Sigma = (1 - X_+)^{-1}$ at $\bar{q} = 0$, with the relevant entries $\Sigma^{11} = \Sigma^{22} = 2/x^2$ and $\Sigma^{33} = 1/x^2$. These expressions are valid in the regime $l/L \ll x$ and will be used here. For general x, L , the finite size form of the vertex correction has to be taken into account, giving e.g. $\Sigma^{22} = (2/x^2)(1 - \tanh(xL/2l)/(xL/2l))$, which then renders Eq. (7) given below finite for $x \rightarrow 0$.

In the regime $\max\{(l/L)^2, \tau/\tau_\phi\} \ll x^2$, we find for the in-plane ($i = 1, 2$) and out-of-plane ($i = 3$) components of the variance

$$\overline{(\delta\chi^{ij})^2} = \left(\frac{e\delta\bar{q}^2}{8\pi^3 v_F} \right)^2 \sum_{n_x=1, n_y=0}^{\infty} s^{ij}(\bar{q}_{n_x}, \bar{q}_{n_y}), \quad (5)$$

where $v_F = p_F/m$ is the Fermi velocity, $\delta\bar{q} = \pi l/L$, and the sum over the $\bar{q}_n \equiv \delta\bar{q}n$ satisfies the mixed boundary conditions for the Diffuson [12] in a finite sample of square size L with two opposite sides attached to the leads. Here, s^{ij} in Eq. (5) are rational functions in $\bar{q}_{n_x}, \bar{q}_{n_y}$ depending parametrically on x, \mathbf{b}, Δ , and the orbital dephasing rate $\phi = \tau/\tau_\phi = 2l^2/L_\phi^2$.

Evaluating s^{ij} for $l/L, l/L_\phi \ll x$ first for $b = \Delta = 0$, and choosing the E-field along x (i.e. $j = 1$) we find

$$s^{i1} = \frac{a_i (4x\Sigma^{ii})^2}{(\bar{q}^2 + 2\phi)^2}, \quad (6)$$

where $a_1 = a_2 = 1$ and $a_3 = 2$. From Eqs. (5), (6) we then obtain $\overline{(\delta\chi^{i1})^2} = (ex\Sigma^{ii}/2\pi^3 v_F)^2 c_2 a_i$, where $c_2 = \sum_{n_x, n_y} \delta\bar{q}^4 / [(n_x^2 + n_y^2)\delta\bar{q}^2 + 2\phi]^2$. To assess the magnitude of this result we compare it to the average of the in-plane susceptibility $\overline{\chi^{21}} = ex/2\pi v_F$ [4]. For the out-of-plane component of the spin fluctuations this yields

$$\frac{\overline{(\delta\chi^{31})^2}}{(\overline{\chi^{21}})^2} = \frac{2c_2}{\pi^4 x^4} = \frac{c_2}{2\pi^4} \frac{\tau_{DP}^2}{\tau^2}, \quad (7)$$

and similarly for the in-plane components. Thus, we see that the relative fluctuations grow with increasing τ_{DP} , where $\tau_{DP} = 2\tau/x^2$ is the D'yakonov-Perel spin relaxation time [28].

Remarkably, for negligible dephasing, i.e. $\phi \ll 1$, one obtains $c_2 \approx 1.51$, and the spin fluctuations $\overline{(\delta\chi^{ij})^2}$ become independent of the sample size. Typical numbers for a GaAs 2DEG (that are consistent with the regime of validity for $L_\phi = 10l$) yield $x = 0.1 \dots 1$ and thus result in large relative fluctuations, $\sqrt{\overline{(\delta\chi^{ij})^2}}/\overline{\chi^{21}} \approx 20 \dots 0.2$. In other words, there exist specific impurity configurations and realistic system parameters that give rise to a large out-of-plane spin polarization in response to a static in-plane electric field.

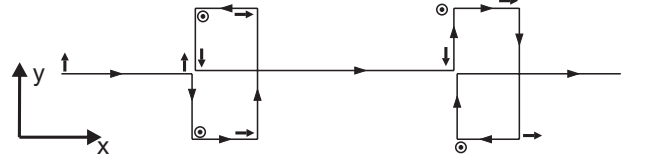


FIG. 3: Example of a propagation path along which an initially y -polarized spin (small arrow) rotates exclusively into the positive out-of-plane z -direction (denoted by circled dots). The spin directions are denoted by small arrows at the left of each segment and result from precession about the instantaneous Rashba spin-orbit field.

To gain physical insight into this result, we consider an electron with spin initially pointing along the y -axis, see Fig. 3. While the electron propagates coherently through the sample, the spin precesses about the intrinsic Rashba SOI field which is in-plane and perpendicular to the propagation direction. As a result of orbital phase coherence the electron propagates along a path that is preferred by constructive interference in the given disorder configuration. Fig. 3 shows an example of such a path and the spin directions associated with the propagation through each segment[33]. Along this entire path the spin can only point up ($+z$ -direction), but never down. Now, if initially the electrons were unpolarized, the net out-of-plane polarization in this case would be cancelled by spins that are initially pointing along the negative y -direction. However, due to the (in-plane) MEE, which itself is subject to strong fluctuations, e.g. due to conductance fluctuations, there is a finite in-plane polarization to begin with. The cancellation is therefore incomplete. These considerations make plausible that disorder configurations exist that give rise to strong out-of-plane spin polarizations.

We next consider the effect of an in-plane magnetic field. For $b = 0$ we see that the terms a) and d) in Eq. (3) contribute equally to the variance. However, for $b \neq 0$ the $1/\bar{q}^2$ -divergence is cut off in the Cooperon and we can approximate Eq. (5) by making use of

$$s_b^{ij} \approx s_{b=0}^{ij} \frac{1}{2} \left[1 + 1/\left(1 + \frac{32(b\tau)^2}{(\bar{q}^2 + 2\phi)x^2} \right) \right], \quad (8)$$

where the first term in Eq. (8) results from the Diffuson contribution (the term containing V_{La}, V_{Ra} in Eq. (3)) which is not affected by (moderate) magnetic fields.

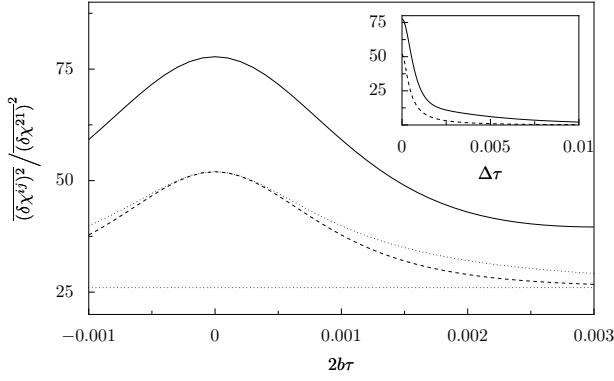


FIG. 4: The relative variance of the out-of-plane spin susceptibility $(\delta\chi^{31})^2 / \delta\chi^{21}{}^2$ is shown as a function of the in-plane magnetic field $2b\tau$ for $x = 0.1$, $L_\phi = 100l$, and sample sizes $L = 100\pi l$ (solid line) and $L = 200\pi l$ (dashed line), *resp.* The low field approximation, Eq. (8), (curved dotted line) and half of the $b = 0$ -value (straight dotted line) are shown for $L = \pi l 100$. Inset: Variance as a function of Δ for $x = 0.1$, $L_\phi = 100l$, and $L = 100\pi l$ (solid line) and $L = 200\pi l$ (dashed line). The suppression of $\delta\chi^{31}$ with increasing b and Δ is described by Eqs. (8) and (9).

Unlike the magnetic field, a difference in energies Δ (e.g. induced by gate voltages) leads to a suppression of all terms contributing to $\delta\chi^2$. This is described by

$$s_{\Delta}^{ij} \approx s_{\Delta=0}^{ij} / \left(1 + \frac{4(\Delta\tau)^2}{(\bar{q}^2 + 2\phi)^2} \right), \quad (9)$$

which gives rise to a correlation scale for susceptibilities at different gate voltages. Indeed, according to Eq. (9), we can regard $\chi(E_F)$ and $\chi(E_F + \Delta)$ as uncorrelated for $\Delta \geq \max\{\phi/\tau, (\pi l/L)^2/\tau\}$.

In conclusion, we find strong mesoscopic fluctuations of the spin-electric susceptibility in a disordered 2DEG due to Rashba SOI, giving rise to a large out-of-plane polarization. The predicted values and dependences on the SOI strength, B-field, dephasing rate, and Fermi energy are well within experimental reach. Such spin-dependent coherence effects, besides being of fundamental interest, might prove useful in spintronics applications aiming at the electrical control of spin polarization.

We thank O. Chalaev, O. Tsyplatyev, and B. Altshuler for discussions. We acknowledge financial support from the Swiss NF and the NCCR Nanoscience Basel.

[1] D. D. Awschalom, D. Loss, and N. Samarth, eds., *Semiconductor Spintronics and Quantum Computation* (Springer, Berlin, 2002).

[2] D. D. Awschalom and M. E. Flatté, *Nature Physics* **3**, 153 (2007).
[3] L. S. Levitov, Y. V. Nazarov, and G. M. Eliashberg, *Zh. Eksp. Teor. Fiz.* **88**, 229 (1985).
[4] V. M. Edelstein, *Solid State Comm.* **73**, 233 (1990).
[5] Y. K. Kato, R. C. Myers, A. C. Gossard, and D. D. Awschalom, *Phys. Rev. Lett.* **93**, 176601 (2004).
[6] Y. K. Kato, R. C. Myers, A. C. Gossard, and D. D. Awschalom, *Nature* **427**, 50 (2004).
[7] Y. K. Kato, R. C. Myers, A. C. Gossard, and D. D. Awschalom, *Appl. Phys. Lett.* **87**, 022503 (2005).
[8] A. Y. Silov et al., *Appl. Phys. Lett.* **85**, 5929 (2004).
[9] D. Stich *et al.*, *Phys. Rev. Lett.* **98**, 176401 (2007).
[10] L. Meier *et al.*, *Nature Phys.* **3**, 650 (2007).
[11] Y. A. Bychkov and E. I. Rashba, *J. Phys. C* **17**, 6039 (1984).
[12] E. Akkermans and G. Montambaux, *Mesoscopic physics of electrons and photons* (Cambridge Univ. Press, 2007).
[13] B. L. Altshuler, *Sov. JETP Lett.* **41**, 648 (1985).
[14] B. L. Altshuler, P. A. Lee, and R. A. Webb, eds., *Mesoscopic Phenomena in Solids* (Elsevier, 1991).
[15] P. A. Lee, A. D. Stone, and H. Fukuyama, *Phys. Rev. B* **35**, 1039 (1987).
[16] D. M. Zumbühl *et al.*, *Phys. Rev. B* **72**, 081305(R) (2005).
[17] J. B. Miller *et al.*, *Phys. Rev. Lett.* **90**, 076807 (2003).
[18] I. L. Aleiner and V. I. Fal'ko, *Phys. Rev. Lett.* **87**, 256801 (2001).
[19] M. Duckheim and D. Loss, *Nature Physics* **2**, 195 (2006); *Phys. Rev. B* **75**, 201305(R) (2007).
[20] O. Chalaev and D. Loss, *Phys. Rev. B* **71**, 245318 (2005); *ibid.* **115352**, **77** (2008).
[21] A. Y. Zyuzin, *Europhys. Lett.* **12**, 529 (1990).
[22] H.-A. Engel, E. I. Rashba, and B. I. Halperin (2006), cond-mat/0603306.
[23] J. Walls and E. Heller, *Nano Letters* **7**, 3377 (2007).
[24] J. H. Bardarson, I. Adagideli, and P. Jacquod, *Phys. Rev. Lett.* **98**, 196601 (2007).
[25] J. J. Krich and B. I. Halperin (2008), arXiv.org:0801.2592.
[26] M. Oestreich, M. Römer, R. J. Haug, and D. Hägele, *Phys. Rev. Lett.* **95**, 216603 (2005).
[27] G. Bergmann, *Phys. Rep.* **107**, 1 (1984).
[28] M. I. D'yakonov and V. I. Perel, *Sov. Phys. Solid State* **13**, 3023 (1972).
[29] We note that Dresselhaus and Rashba SOI give the same results since the corresponding Hamiltonians are unitarily related [20].
[30] The B-field breaks time-reversal invariance and leads to additional terms in Eq. (2). However, their contribution to $(\delta\chi^{ij})^2$ is negligible for the small B-fields $b\tau \approx \sqrt{x^2\phi}$ relevant for C, see Eq. (8).
[31] Note that $G_E^R G_E^R (G_E^A G_E^A)$ drops out in Eq. (2) due to the identity $G_E^{R/A} v_j G_E^{R/A} = -i[x_j, G_E^{R/A}]/\hbar$.
[32] E.g., $V_{Rd}^{\kappa\nu}[\sigma^i, v_m] = (dk^T)^{\kappa l} (\bar{d} k k^T)^{ij} k^{\nu r} V[\sigma^l, \sigma^j, \sigma^r, v_m]$, where $k^{\mu l} = \text{tr}\{\sigma^2 \sigma^\mu \sigma^l\}/2$ and $d(\bar{d}) = \text{diag}(1, -1, -1, -1, +1(-1), +1(-1))$.
[33] Note that along each segment the electron undergoes many scatterings for $x = l/l_{SO} \ll 1$.